REPORT DOCUMENTATION PAGE

Public reporting burden for this collection of information is estimated to average 1 hour per response, including the time for reviewing instructions, searching existing data sources, gathering and maintaining the data needed, and completing and reviewing this collection of information. Send comments regarding this burden estimate or any other aspect of this collection of information, including suggestions for reducing this burden to Department of Defense, Washington Headquarters Services, Directorate for Information Operations and Reports (0704-0188), 1215 Jefferson Davis Highway, Suite 1204, Arlington, VA 22202-4302. Respondents should be aware that notwithstanding any other provision of law, no person shall be subject to any penalty for failing to comply with a collection of information if it does not display a currently valid OMB control number. PLEASE DO NOT RETURN YOUR FORM TO THE ABOVE ADDRESS.

1. REPORT DATE (DD-MM-YYYY)	2. REPORT TYPE	3. DATES COVERED (From - To)
06-11-1997	Paper	

4. TITLE AND SUBTITLE	5a. CONTRACT NUMBER
The Influence of Combustion Noise on Acoustic Instabilities	
	5b. GRANT NUMBER
	5c. PROGRAM ELEMENT NUMBER

6. AUTHOR(S)	5d. PROJECT NUMBER
V.S. Burnely; F.E.C. Culick	3058
	5e. TASK NUMBER
	RF9A
	5f. WORK UNIT NUMBER

7. PERFORMING ORGANIZATION NAME(S) AND ADDRESS(ES) AND ADDRESS(ES)	8. PERFORMING ORGANIZATION REPORT
Air Force Research Laboratory (AFMC) AFRL/PRS 5 Pollux Drive Edwards AFB CA 93524-7048	

9. SPONSORING / MONITORING AGENCY NAME(S) AND ADDRESS(ES)	10. SPONSOR/MONITOR'S ACRONYM(S)
Air Force Research Laboratory (AFMC) AFRL/PRS 5 Pollux Drive Edwards AFB CA 93524-7048	
	11. SPONSOR/MONITOR'S NUMBER(S) AFRL-PR-ED-TP-1998-011

12. DISTRIBUTION / AVAILABILITY STATEMENT
Approved for public release; distribution unlimited.

13. SUPPLEMENTARY NOTES

14. ABSTRACT

20020115 087

15. SUBJECT TERMS

16. SECURITY CLASSIFICATION OF:			17. LIMITATION OF ABSTRACT	18. NUMBER OF PAGES	19a. NAME OF RESPONSIBLE PERSON Doug Talley
a. REPORT Unclassified	b. ABSTRACT Unclassified	c. THIS PAGE Unclassified	A		19b. TELEPHONE NUMBER (include area code) (661) 275-6174

The Influence of Combustion Noise on Acoustic Instabilities

V. S. Burnley*

U. S. Air Force Research Laboratory, Edwards Air Force Base, California 93524

and

F. E. C. Culick[†]

California Institute of Technology, Pasadena, California 91125

Abstract

Although flows in combustors contain considerable noise, arising from several kinds of sources, there is a sound basis for treating organized oscillations as distinct motions. That has been an essential assumption incorporated in virtually all treatments of combustion instabilities. However, certain characteristics of the organized or deterministic motions seem to have the nature of stochastic processes. For example, the amplitudes in limit cycles always exhibit a random character and even the occurrence of instabilities seems occasionally to possess some statistical features. Analysis of nonlinear coherent motions in the presence of stochastic sources is therefore an important part of the theory. We report here a few results for organized oscillations in the presence of noise. The most significant deficiency of this work is that, owing to the low level of current understanding, the stochastic sources of noise are modeled in *ad hoc* fashion and

---

*Research Engineer, Propulsion Directorate. Member AIAA.

[†]Richard L. and Dorothy M. Hayman Professor of Mechanical Engineering and Professor of Jet Propulsion. Fellow AIAA.

are not founded on a solid physical basis appropriate to combustion

chambers.

Nomenclature

a	= speed of sound
f	= nonlinear functional arising from the boundary conditions
F_n	= forcing function of the nth acoustic mode
h	= nonlinear functional arising from the conservation equations
k_n	= wavenumber of the nth acoustic mode
$\hat{n}$	= unit outward normal vector
p	= pressure
r_n	= magnitude of time-dependent amplitude $\eta_n(t)$, Eq. (20)
s	= entropy
$\boldsymbol{u}$	= velocity
α_n	= linear growth rate of the nth acoustic mode
η_n	= time-dependent amplitude of the nth acoustic mode
ξ	= parametric stochastic excitation associated with pressure
ξ^v	= parametric stochastic excitation associated with velocity
Ξ	= external stochastic excitation
ρ	= density
σ	= noise intensity
τ_c	= correlation time
θ_n	= linear frequency shift of the nth acoustic mode
ϕ_n	= phase of the time-dependent amplitude $\eta_n(t)$, Eq. (20)
$\psi_n(\boldsymbol{r})$	= mode-shape of the nth acoustic mode
ω_n	= frequency of the nth acoustic mode
$\boldsymbol{\Omega}$	= vorticity
Subscripts	
$(\ )_a$	= acoustic waves
$(\ )_s$	= entropy waves
$(\ )_\Omega$	= vorticity waves
Superscripts	
NL	= nonlinear
$^-$	= mean quantity
$'$	= fluctuating quantity
$\cdot$	= time derivative

2

1 Introduction

Combustion chambers are inherently noisy environments. This is apparent from inspection of the power spectra of pressure records from test firings, as well as from simply listening to the tests. When an organized oscillation, i.e., a combustion instability, is present, the power spectrum exhibits well-defined peaks in addition to background noise over the entire range of frequencies. Substantial noise sources in rocket motors include flow separation, turbulence, and combustion processes. It is expected that the presence of noise will affect in some way the amplitudes and possibly the qualitative behavior of coherent oscillations. Nonetheless, there is a sound basis for treating instabilities as distinct motions, and much progress has been made using this assumption.

There are two general types of coherent oscillations which commonly occur in combustion chambers: spontaneous oscillations and pulsed oscillations. A spontaneous oscillation occurs when the system is linearly unstable. As a result, any perturbation of the system grows exponentially in time. Under the influence of nonlinear effects, the pressure field may reach a periodic motion, or limit cycle. This type of instability is also known as an intrinsic instability or a soft excitation. In the field of dynamical systems, the change of behavior from a linearly stable steady state to a stable path of periodic solutions is called a supercritical bifurcation.

A pulsed oscillation, on the other hand, is a true nonlinear instability of a linearly stable system. Small perturbations in the pressure field decay exponentially to zero, while larger perturbations may lead to stable or unstable periodic motions.

Common terminology used to describe this type of oscillation includes triggered instability, hard excitation, and subcritical bifurcation. Previous works, e.g., Yang et al.,[1] Paparizos and Culick,[2] and Jahnke and Culick,[3] have convincingly shown that nonlinear gasdynamics alone does not contain the possibility of pulsed oscillations. Part of the purpose of the present investigation is to determine if noise processes could be responsible for the occurrence of pulsed oscillations.

Culick et al.[4] studied the influence of noise on combustion instabilities, but only for a very simple case: two acoustic modes with noise present only in the first mode. In addition, the formulation was flawed, and the form of the resulting noise terms is not quite correct. Clavin et al.[5] studied the influence of turbulence on instabilities in liquid rocket motors. Using only one mode in the analysis and third-order nonlinearities, it was reported that the inclusion of noise can lead to the possibility of triggering. It is a well-known result that a single third-order equation may produce a subcritical bifurcation. When more acoustic modes are considered, this may not be the case, as demonstrated by Yang et al.[1] for third-order gasdynamics. Therefore, the results of Clavin et al. may not be applicable in general.

The present analysis is an extension of the previous work by Culick et al.[4] The approximate analysis used here has been covered in many other works, so only a brief overview of the method is presented; for more details, see, e.g., the review by Culick.[6] Then, we will decompose the flow field into acoustic and non-acoustic parts based on the approach followed by Chu and Kovásznay.[7] That tactic produces a formal representation of the noise terms in the governing equations. Finally, we will simplify the equations in order to study more conveniently the possible influences of noise on

4

combustion instabilities.

2 Development of the Approximate Analysis

In order to keep the analysis as general as possible, the formulation begins with the
conservation equations for two-phase flow. These equations are then rewritten in an
equivalent form for a single medium having the mass-averaged properties of the two
phases. Subsequently, a wave equation for the pressure is developed, along with the
corresponding boundary condition.

$$\nabla^2 p' - \frac{1}{\bar{a}^2}\frac{\partial^2 p'}{\partial t^2} = h \tag{1}$$

$$\hat{\boldsymbol{n}} \cdot \nabla p' = -f \tag{2}$$

The functions h and f are linear and nonlinear functions of the pressure and velocity
perturbations. As an approximation, these perturbations are expanded as a synthesis
of classical acoustic modes with time-varying amplitudes,

$$p'(\boldsymbol{r}, t) = \bar{p}\sum_{n=1}^{\infty} \eta_n(t)\psi_n(\boldsymbol{r}) \tag{3}$$

$$\boldsymbol{u}'(\boldsymbol{r}, t) = \sum_{n=1}^{\infty} \frac{\dot{\eta}_n(t)}{\bar{\gamma}k_n^2}\nabla\psi_n(\boldsymbol{r}) \tag{4}$$

where ψ_n is the mode shape and $\eta_n(t)$ is the time-dependent amplitude of the nth
classical acoustic mode. After substituting Eq. (3) in Eq. (1), the equations are
spatially averaged, resulting in a system of ordinary differential equations describing

the amplitudes of the acoustic modes.

$$\frac{d^2\eta_n}{dt^2} + \omega_n^2\eta_n = F_n \tag{5}$$

where $\omega_n = \bar{a}k_n$ and

$$F_n = -\frac{\bar{a}^2}{\bar{p}E_n^2}\left\{\int \psi_n h dV + \oint \psi_n f dS\right\} \tag{6}$$

Thus, the problem is reduced to solving for the amplitudes, $\eta_n(t)$. This approach is very general and can accommodate all damping and amplification mechanisms. The most difficult part of the problem is in the identification and modeling of the important physical processes.

3 Splitting the Unsteady Flow Field Into Acoustic, Vortical, and Entropic Modes of Propagation

Fluctuations in a compressible fluid can be decomposed into three types of waves: acoustic waves, vorticity waves, and entropy waves. A thorough discussion of this idea is presented by Chu and Kovásznay.[7] In the limit of small amplitudes, the three types of waves propagate independently in a uniform mean flow, but are coupled when the mean flow is non-uniform.[8] For example, the pressure in an acoustic wave is changed slightly by the presence of a vorticity or entropy wave if the mean flow is not uniform. Coupling between the types of waves may also occur at the boundaries of the chamber.

6

Although noise is detected as pressure waves, the *sources* of noise are associated with the presence of vorticity fluctuations (e.g., turbulence, flow separation, etc.) and entropy or non-isentropic temperature fluctuations. Therefore, decomposing the unsteady flow field into the three types of waves allows both noise and acoustic instabilities to be handled in the same analytical framework discussed in Sec. 1. The contributions from vorticity and entropy waves appear as additional force terms on the right-hand side of the acoustic equation.

Following the analysis of Chu and Kovásznay,[7] the thermodynamic and kinematic variables can be written as sums of fluctuations in the three waves as follows.

$$p' = p'_a + p'_\Omega + p'_s \tag{7}$$

$$\Omega' = \Omega'_a + \Omega'_\Omega + \Omega'_s \tag{8}$$

$$s' = s'_a + s'_\Omega + s'_s \tag{9}$$

$$u' = u'_a + u'_\Omega + u'_s \tag{10}$$

In general, all of the fluctuations will be nonzero, but not all terms are of the same order. If we restrict the analysis to small amplitude motions, the three waves have the following characteristics:[7]

$(\ )_a$ acoustic waves: pressure and velocity fluctuations, no entropy change

$(\ )_\Omega$ vorticity waves: velocity fluctuations, no pressure or entropy changes

$(\ )_s$ entropy waves: entropy and velocity fluctuations, no pressure change

Thus, to zeroth-order, the fluctuations in the three waves are given by

$$p' = p'_a \tag{11}$$

$$\Omega' = \Omega'_\Omega \tag{12}$$

$$s' = s'_s \tag{13}$$

$$u' = u'_a + u'_\Omega + u'_s \tag{14}$$

An equation for the density fluctuation is obtained by expanding the formula for the entropy of a perfect gas.

$$\frac{\rho'}{\bar{\rho}} = \frac{1}{\bar{\gamma}}\frac{p'_a}{\bar{p}} - \frac{1}{\bar{c}_p}s' \tag{15}$$

As an approximation to the acoustic pressure and velocity perturbations, we will once again use a superposition of the classical acoustic modes so that

$$p'_a = \bar{p}\sum_{n=1}^{\infty} \eta_n(t)\psi_n(\boldsymbol{r}) \qquad u'_a = \sum_{n=1}^{\infty} \frac{\dot{\eta}_n(t)}{\bar{\gamma}k_n^2}\nabla\psi_n(\boldsymbol{r})$$

Substitution of Eq. (11) in the left-hand side of the nonlinear wave equation (1), followed by application of Galerkin's method, leads to a set of coupled nonlinear oscillator equations.

$$\ddot{\eta}_n + \omega_n^2\eta_n = F_n \tag{16}$$

8

where[8]

$$-\frac{\bar{p}E_n^2}{\bar{a}^2}F_n = \bar{\rho}I_1 + \frac{1}{\bar{a}^2}I_2 + \bar{\rho}I_3 + \frac{1}{\bar{a}^2}I_4$$
$$+ \int \bar{\rho}\frac{\partial \boldsymbol{u}'}{\partial t}\cdot\hat{\boldsymbol{n}}dS - \int\left[\frac{1}{\bar{a}^2}\frac{\partial \mathcal{P}'}{\partial t}\psi_n + \boldsymbol{\mathcal{F}}'\cdot\nabla\psi_n\right]dV \quad (17)$$

and

$$I_1 = \int (\bar{\boldsymbol{u}}\cdot\nabla\boldsymbol{u}' + \boldsymbol{u}'\cdot\nabla\bar{\boldsymbol{u}})\cdot\nabla\psi_n dV \qquad I_2 = \frac{\partial}{\partial t}\int(\bar{\gamma}p'\nabla\cdot\bar{\boldsymbol{u}} + \bar{\boldsymbol{u}}\nabla\cdot p')\psi_n dV$$

$$I_3 = \int\left(\boldsymbol{u}'\cdot\nabla\boldsymbol{u}' + \frac{\rho'}{\bar{\rho}}\frac{\partial \boldsymbol{u}'}{\partial t}\right)\cdot\nabla\psi_n dV \qquad I_4 = \frac{\partial}{\partial t}\int(\bar{\gamma}p'\nabla\cdot\boldsymbol{u}' + \boldsymbol{u}'\cdot\nabla p')\psi_n dV$$

In the original development of the approximate analysis, the zeroth-order approximations for the pressure and velocity were used to evaluate F_n. The same idea will be applied here, although additional contributions to the velocity fluctuation from coupling to vorticity and entropy waves will be included. Once these quantities are substituted in the right-hand side, the set of forced oscillator equations eventually takes the general form (see Burnley[9] for details):

$$\ddot{\eta}_n + \omega_n^2\eta_n = 2\alpha_n\dot{\eta}_n + 2\omega_n\theta_n\eta_n - \sum_{i=1}^{\infty}\sum_{j=1}^{\infty}[A_{nij}\dot{\eta}_i\dot{\eta}_j + B_{nij}\eta_i\eta_j]$$
$$+ (F_n)_{\text{other}}^{\text{NL}} + \sum_{i=1}^{\infty}[\xi_{ni}^v\dot{\eta}_i + \xi_{ni}\eta_i] + \Xi_n \quad (18)$$

This system of equations is very complex with many free parameters. For instance, if we truncate the system to N modes, there are $2N$ linear parameters and an additional $2N^2 + N$ unknown functions. In order to simplify the equations somewhat,

9

we will therefore neglect cross-coupling terms in ξ_{ni}^v and ξ_{ni}, i.e., terms with $n \neq i$. These terms may turn out to be important, but neglecting them will allow for easier initial computation of results and will suffice for the purposes here. The simplified set of equations is

$$\ddot{\eta}_n + \omega_n^2 \eta_n = 2\alpha_n \dot{\eta}_n + 2\omega_n \theta_n \eta_n - \sum_{i=1}^{\infty} \sum_{j=1}^{\infty} [A_{nij} \dot{\eta}_i \dot{\eta}_j + B_{nij} \eta_i \eta_j]$$
$$+ (F_n)_{\text{other}}^{\text{NL}} + \xi_n^v(t) \dot{\eta}_n + \xi_n(t) \eta_n + \Xi_n(t) \quad (19)$$

4 Modeling of the Stochastic Sources

The problem has now been reduced to solving Eq. (19) for the time-dependent amplitudes $\eta_n(t)$ which are subjected to additive and multiplicative noise. The source terms $\xi_n^v(t)$, $\xi_n(t)$, and $\Xi_n(t)$ represent stochastic processes of some sort and are responsible, in this formulation, for the background noise found in the power spectra of test firings. The problem of modeling these processes, however, remains. This requires specification of both the spatial and temporal distribution of the velocity and the entropy. At the present time, no models exist for these fluctuations.

There are several other paths that can be followed at this point which include obtaining approximate representations for the velocity and entropy fluctuations based on experimental data or numerical simulations. The approach that will be taken here is to assume forms for the source terms which are based on observations of experiments. By inspection of the pressure traces of test firings, it is apparent that the stochastic processes in real systems are broadband with very small correlation

10

times*, τ_c. The limit $\tau_c \to 0$ represents a delta correlated process, i.e., a process which is totally uncorrelated with itself. It is thus interesting to study this limiting case and assume that the stochastic terms are represented by *white noise.*

The definition of a white noise process is a process whose spectral density is flat, i.e., all frequencies are present at the same amplitude. Although such a process cannot occur in a real system, white noise can be a very useful tool for studying real processes which have very small correlation times compared to the macroscopic times of the system. This is true of the random processes and systems of interest.[4] Therefore, we will approximate ξ_n^v, ξ_n, and Ξ_n by mutually independent white noise processes with zero mean values and intensities denoted by $\sigma_n^{\xi^v}$, σ_n^{ξ}, and σ_n^{Ξ}.

An example of a simulation with white noise excitations is presented in Fig. 1. A sample trace of the pressure at the head end of the combustion chamber is shown along with the corresponding normalized spectrum. Inspection of the spectrum shows peaks at distinct frequencies which are associated with an acoustic instability, along with broadband background noise. This is characteristic of actual test data of a case when an instability is present. For the simulation shown in Fig. 1, as well as all other results presented here, the values given in Table 1 will be used for the linear parameters of the system.

---

*The correlation time is the time above which the autocorrelation function is zero. This is a measure of the dependence of the process on its past.

n	1	2	3	4
$\alpha_n(\text{sec}^{-1})$	free	-324.8	-583.6	-889.4
$\theta_n(\text{rad/sec})$	12.9	46.8	-29.3	-131.0

Table 1: Linear growth rates and frequency shifts

5 Results

Since we are interested in nondeterministic systems, it is natural to use the probability density functions of the amplitudes of acoustic modes to investigate the dynamics of the system. In particular, we will use the amplitude r_n which is defined in the following equation.

$$\eta_n(t) = r_n(t)\cos(\omega_n t + \phi_n(t)) \tag{20}$$

Using r_n instead of η_n, any quantitative changes which occur in the solution will be more apparent since r_n is a measure of the magnitude of the oscillation. Note that this change of variables from $(\eta_n, \dot{\eta}_n)$ to (r_n, ϕ_n) will cause a shift in the expected value. This is obvious from the definition of r_n, which is defined as $\sqrt{\eta_n^2 + \dot{\eta}^2/\omega_n^2}$

A Monte-Carlo method will be used to obtain an approximation to the probability density functions of the acoustic amplitudes. In this method, a series of numerical "experiments" is conducted, usually in the same manner that one would conduct actual experiments. After the flow field has become well-developed (say after 1000 periods of the fundamental mode or so), the amplitudes of the acoustic modes are sampled. The results are then used to construct histograms which, after normalization, approx-

imate the instantaneous probability density functions of the modal amplitudes. The approximation becomes better as the number of experiments is increased.

In the current study, each Monte-Carlo simulation will consist of 10000 numerical experiments. The linear parameters will be fixed throughout a series of experiments, while the initial conditions for the simulations will be varied systematically. In particular, a square initial pulse which is nonzero from $0 \leq x/L \leq .25$ will be used. The size of the pressure pulse $p'/\bar{p}$ will be varied from 0 to .2 linearly so as to include most likely values.

For the initial results, we will use the simplest possible set of equations. The system will be truncated to two modes with noise included explicitly only in the fundamental mode. We will also assume initially that the only nonlinear contributions are associated with gasdynamics. These simplifications were used by Culick et al.[4] and will allow the effects of each type of stochastic excitation to be determined. We will relax these simplifications later in this section when nonlinear contributions from combustion are also included.

5.1   The Effects of an External Excitation

The term Ξ_1 is an external excitation, i.e., it does not depend on the current state of the system. As a result, this type of excitation does not change the qualitative behavior of the system from that of the original deterministic system,[10] i.e., no matter how large the intensity, the addition of an external excitation does not affect the locations or types of attractors in the system. Instead, an external excitation provides only a random perturbation from these states; the dynamics of the system are constantly

acting to bring a stable system back to a state of equilibrium.

To understand better the effects of an external excitation, it is useful to treat the deterministic case as the limit of $\sigma_1^{\bar{\Xi}} \to 0$. For a deterministic system with nonlinear contributions from gasdynamics only, the stationary probability density functions will be delta functions in terms of r_n. For example, the probability density functions of a linearly stable system without random perturbations will be delta functions at $r_n = 0$ for all n. When an external excitation is introduced, the effect is to shift the mean value of the amplitude r_n to a nonzero value (due to the change of variables) and increase the variance of the oscillation such that a broader range of values is likely. This broadening effect can be seen in Figs. 2 and 3 for linearly stable and linearly unstable systems, respectively.

To demonstrate the effect of noise intensity on the probability density, the value used in Fig. 3 was doubled, and the result is plotted in Fig. 4. As the intensity of the noise increases, the variance of the probability density function increases so that a larger range of modal amplitudes is likely. The mean value of the amplitude, however, remains unchanged.

Another interesting aspect of an external excitation can be seen if we look at a sample pressure history and spectral density for a linearly stable system with an external excitation. At first inspection of Fig. 5, it might appear that the system is linearly unstable due to the very low amplitude oscillation. The data shown in Fig. 5 is, however, for a stable system. It happens that an external excitation, though random, will excite the natural acoustic modes of the chamber such that a low amplitude fluctuation is present. The energy provided by the external excitation Ξ_1 is most eas-

14

ily transferred into the fundamental acoustic mode because this excitation appears in the equation for the fundamental mode. Therefore, the system oscillates at the fundamental frequency of the chamber. However, in terms of dynamical systems theory, the system is still linearly stable, and the dynamics of the system always act to bring the chamber back to a state of rest. Recently, in analyzing data similar to this, Malhotra and Flandro[11] suggested that the system was linearly unstable due to the presence of a very low amplitude oscillation. We believe that the system being analyzed by Flandro was actually linearly stable and that the low amplitude oscillation was actually caused by the noise processes which are always present in real systems.

5.2 The Effects of a Noisy Linear Growth Rate

Unlike the external excitations covered in the previous section, the parametric excitations $\xi_1^v \dot{\eta}_1$ and $\xi_1 \eta_1$ depend upon the current state of the system. In a more illuminating form, the system (19) can be rewritten as

$$
\ddot{\eta}_1 + \omega_1^2 \eta_1 = 2 \left(\alpha_1 + \frac{1}{2} \xi_1^v \right) \dot{\eta}_1 + 2\omega_1 \left(\theta_1 + \frac{1}{2\omega_1} \xi_1 \right) \eta_1 + (F_1)^{\mathrm{NL}} + \Xi_1(t)
$$

$$
\ddot{\eta}_2 + \omega_2^2 \eta_2 = 2\alpha_2 \dot{\eta}_2 + 2\omega_2 \theta_2 \eta_2 + (F_2)^{\mathrm{NL}} \tag{21}
$$

By inspection of the above system, it is easy to see that ξ_1^v is a random perturbation of the linear growth rate of the first acoustic mode. Similarly, ξ_1 is a random perturbation of the linear frequency shift. In this section, we will study the effects of a noisy linear growth rate on the dynamics of the system, while the effects of a noisy linear frequency shift will be handled in the next section.

There are two main effects caused by the noisy linear growth rate ξ_1^v. The first is a result of approximating a real noise process by white noise. Since no real process is truly white, the system will have a small but finite memory, i.e., there will be some correlation between the noise and the system. This correlation is taken into account by the Stratonovich representation through its definition of the stochastic integral.[10] As a result, the linear growth rate is increased to an apparent value given by

$$(\alpha_1)_{\text{apparent}} = \alpha_1 + \left(\frac{\sigma_1^{\xi^v}}{2}\right)^2 \tag{22}$$

Thus, one effect of a noisy linear growth rate is to shift the bifurcation diagram by an amount proportional to the square of the intensity of the noise. This is known as noise-induced drift.[10] The second effect of the noisy linear growth rate is similar to the effect of an external excitation. It is basically a disorganizing effect which tends to spread the peak of the probability density functions about the mean value.

This type of parametric excitation was studied by Horsthemke and Lefever[10] on a first-order nonlinear equation. In that study, the Verhulst model with a noisy growth rate was shown to have two transition points at which the probability density function changes qualitatively. Thus, three ranges of linear growth rate which produce three different types of probability density function were found. Three qualitatively different types of probability density functions are also found in our system. However, it is difficult to predict the exact location of the transitions due to the highly nonlinear nature of the system of equations.

For highly stable systems, i.e., $\alpha_1 \ll 0$ sec^{-1}, the attractor at $r_n = 0$ is so strong

that the solution will always be drawn back to this steady state. Once this state is reached, the parametric excitation no longer affects the system. As a result, the stationary probability density functions for highly stable systems will be delta functions at $r_n = 0$ for all n. For mildly stable and/or unstable systems, a second type of probability density function occurs. While the most probable value is still zero, the mean value is not. This type of probability density function was shown previously in the study by Culick et al.[4] An example is shown here in Fig. 6 for $\alpha_1 = -8$ sec^{-1}.

The final type of probability density occurs in systems which are highly unstable. In that case, the linear growth rate α_1 is so large that it is unlikely that the noise will be strong enough for a sufficient amount of time to drive the solution back to the trivial state. Therefore, both the mean value and the most probable value are nonzero. Figure 7 shows an example of such a probability density function for $\alpha_1 = 25$ sec^{-1}. Note that the mean value is shifted slightly from the deterministic value of 0.07. This is an example of noise-induced drift.

For the deterministic system with nonlinear contributions from gasdynamics only, two qualitatively different regions are found: one region of stable steady states and one region of stable limit cycles. When noise of a parametric nature is added, three distinct regions arise because $r_n = 0$ is a stationary point of the system for all values of α_1 and σ^{ξ^v}.[10] However, if an external excitation is also included in the system, $r_n = 0$ is no longer a stationary state (although it is still an attractor), and only two different regions are found.

5.3 The Effects of a Noisy Linear Frequency Shift

The effects of a noisy linear frequency shift are very similar to the effects of ξ_1^v, so only a brief discussion is necessary. Since ξ_1 is also a parametric excitation, a stationary state occurs once again for $r_n = 0$, and three regions of distinct types of probability density functions are produced. The three types are qualitatively similar to those in the previous section, although the transition points may occur at different values of α_1. A sample probability density function for a linearly unstable system with a noisy linear frequency shift is plotted in Fig. 8.

5.4 The Effects of Noise and Nonlinear Combustion

In the previous sections involving nonlinear contributions from gasdynamics only, no cases were found which are consistent with the qualitatively different behaviour of triggering, i.e., nonlinear instabilities in a linearly stable system. As no examples of triggering were found for the case of noise and nonlinear gasdynamics, a model of nonlinear combustion which has previously been shown[12] to provide the possibility of triggering will be included in the analysis in order to determine the effects of noise on a deterministic system which has multiple stable stationary states for the same value of α_1.

The threshold velocity model is an ad hoc model which is based on the idea of velocity coupling with a threshold value below which the effects of nonlinear combustion are not felt. Threshold effects have been observed in experimental investigations of velocity coupling. Ma et al.[13] found a threshold acoustic velocity above which the

18

mean mass flux increased linearly with the Reynold's number of the acoustic fluctuations. Below the threshold value, the mean mass flow was approximately constant. It was determined that the increased mass flux is a result of increased heat transfer to the surface after transition to turbulent flow had occurred.

The form of the threshold velocity model is given by

$$\dot{m}' = \bar{\dot{m}} R_{vc} F(u') \tag{23}$$

where the function $F(u')$ is shown in Fig. 9. This function introduces a dead zone in which the nonlinear contributions from combustion do not affect the system. When the amplitudes of oscillations become larger than the chosen threshold value u_t, the nonlinear effects are then felt. The threshold velocity model can be included in the analysis using the term $(F_n)_{\text{other}}^{\text{NL}}$; the details of this are given in Burnley.[9]

When nonlinear combustion is added to the stochastic system (19), the resulting probability density functions can be quite different, as one might expect. In a previous investigation, we have shown that the threshold velocity model can produce regions of possible triggering in which two stable solutions exist simultaneously. In a stochastic system, this corresponds to a bimodal probability density function such that there is a high probability of low and high amplitudes and a low probability of intermediate values.

For the parametric values in the threshold velocity model, we will use a nondimensional threshold velocity of $u_t/a = 0.03$ and $R_{vc} = 7.8$. Using these values, the bifurcation diagram for the deterministic system is shown in Fig. 10. This diagram

19

will be useful in the discussion of results. In addition, the following values were chosen for the intensities of the stochastic sources: $\sigma_n^{\xi^\nu} = 0.005$ sec$^{-3/2}$, $\sigma_n^\xi = 0.025$ sec$^{-1/2}$, and $\sigma_n^\Xi = 0.0005$ sec$^{-3/2}$, for $n = 1, 2$. The parameter α_1 will be varied while all other parametric values remain fixed. By changing this parameter, we will demonstrate a variety of the possible forms of the probability density functions.

From inspection of Fig. 10, we see that the region of possible triggering begins at approximately $\alpha_1 = -30$ sec^{-1} for the deterministic system. Below this value, the deterministic system is stable to any size perturbation. To illustrate the effect of noise on such a system, a linear growth rate of -35 sec^{-1} was chosen. Figure 12a shows the resulting probability density function for the first acoustic mode. For this case, the attractor of the deterministic system, i.e., the trivial steady state, is so strong that the amplitudes never reach large values. Therefore, the parametric excitations, i.e., ξ_n^ν and ξ_n, have a very small effect on the system. Most of the noise contribution is a result of the external excitations, Ξ_n.

As the linear growth rate is increased to a value above -30 sec^{-1}, we enter the region of possible triggering for the deterministic system where an additional attractive state is present. Three values of α_1 were chosen in order to show how the probability density of the fundamental mode changes throughout this region. As the value of α_1 is varied, the regions of attraction of the stationary states will change. This will have a noticeable effect on the probability density functions.

The first value of α_1 is very close to the lower boundary of the region of possible triggering. For a value of $\alpha_1 = -25$ sec^{-1}, Fig. 12b shows the probability density function of the fundamental mode. The low amplitude attractive state is dominant

I: Longitudinal Modes", *AIAA 25th Aerospace Sciences Meeting*, AIAA Paper 87-1873, 1987.

[2] Paparizos, L. and Culick, F. E. C., "The Two-Mode Approximation to Nonlinear Acoustics in Combustion Chambers. I. Exact Solutions for Second Order Acoustics", *Combustion Science and Technology*, Vol. 65, No. 5, 1989, pp. 39–65.

[3] Jahnke, C. C. and Culick, F. E. C., "An Application of Dynamical Systems Theory to Nonlinear Combustion Instabilities", *Journal of Propulsion and Power*, Vol. 10, No. 4, 1994, pp. 508–517.

[4] Culick, F. E. C., Paparizos, L., Sterling, J., and Burnley, V., "Combustion Noise and Combustion Instabilities in Propulsion Systems", *Proceedings of the AGARD Conference on Combat Aircraft Noise*, AGARD CP 512, 1992.

[5] Clavin, P., Kim, J. S., and Williams, F. A., "Turbulence-Induced Noise Effects on High-Frequency Combustion Instabilities", *Combustion Science and Technology*, Vol. 96, 1994, pp. 61–84.

[6] Culick, F. E. C., "Some Recent Results for Nonlinear Acoustics in Combustion Chambers", *AIAA Journal*, Vol. 32, No. 1, 1994, pp. 146–169.

[7] Chu, B.-T. and Kovásznay, L. S. G., "Nonlinear Interactions in a Viscous Heat-conducting Compressible Gas", *Journal of Fluid Mechanics*, Vol. 3, No. 5, 1958, pp. 494–514.

[8] Culick, F. E. C., "Nonlinear Acoustics in Combustion Chambers With Stochastic

Sources", Guggenheim Jet Propulsion Center, California Institute of Technology, Documents on Active Control of Combustion Instabilities CI95-6, 1995.

[9] Burnley, V. S., *Nonlinear Combustion Instabilities and Stochastic Sources*, PhD thesis, California Institute of Technology, Pasadena, CA, 1996.

[10] Horsthemke, W. and Lefever, R., *Noise-Induced Transitions*, Springer-Verlag, Berlin, 1984.

[11] Malhotra, S. and Flandro, G. A., "On Nonlinear Combustion Instability", *33rd AIAA/ASME/SAE/ASEE Joint Propulsion Conference*, AIAA Paper 97-3250, 1997.

[12] Burnley, V. S., Swenson, G., and Culick, F. E. C., "Pulsed Instabilities in Combustion Chambers", *31st AIAA/ASME/SAE/ASEE Joint Propulsion Conference*, AIAA Paper 95-2430, 1995.

[13] Ma, Y., Moorhem, W. K. Van, and Shorthill, R. W., "Experimental Investigation of Velocity Coupling in Combustion Instability", *Journal of Propulsion and Power*, Vol. 7, No. 5, 1991, pp. 692–699.

[14] Flandro, G. A., "Effects of Vorticity on Rocket Combustion Stability", *Journal of Propulsion and Power*, Vol. 11, No. 4, 1995, pp. 607–625.

[15] Roh, T.-S., Tseng, I.-S., and Yang, V., "Effects of Acoustic Oscillations in Flame Dynamics of Homogeneous Propellants in Rocket Motors", *Journal of Propulsion and Power*, Vol. 11, No. 4, 1995, pp. 640–650.
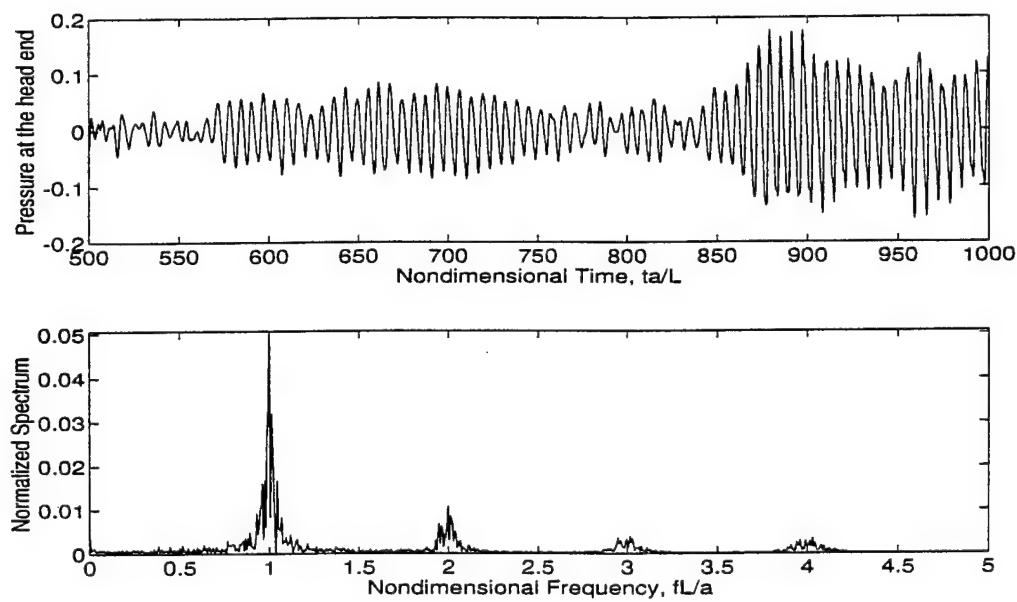
Figure 1: Sample pressure trace and spectrum for a simulation
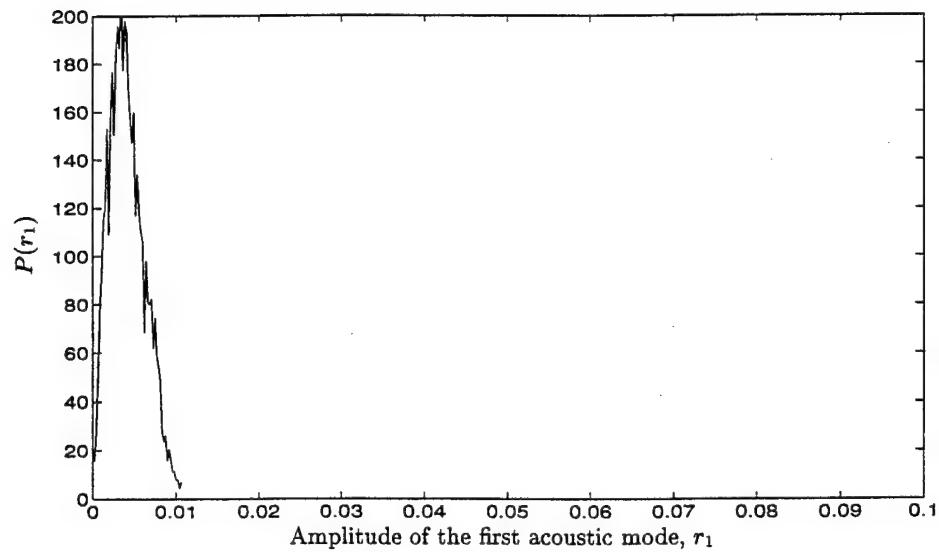
Figure 2: The influence of an external excitation of the fundamental mode only on a linearly stable system; 2 modes, $\sigma_1^{\Xi} = 0.0005$ sec$^{-3/2}$, $\alpha_1 = -25$ sec^{-1}

25
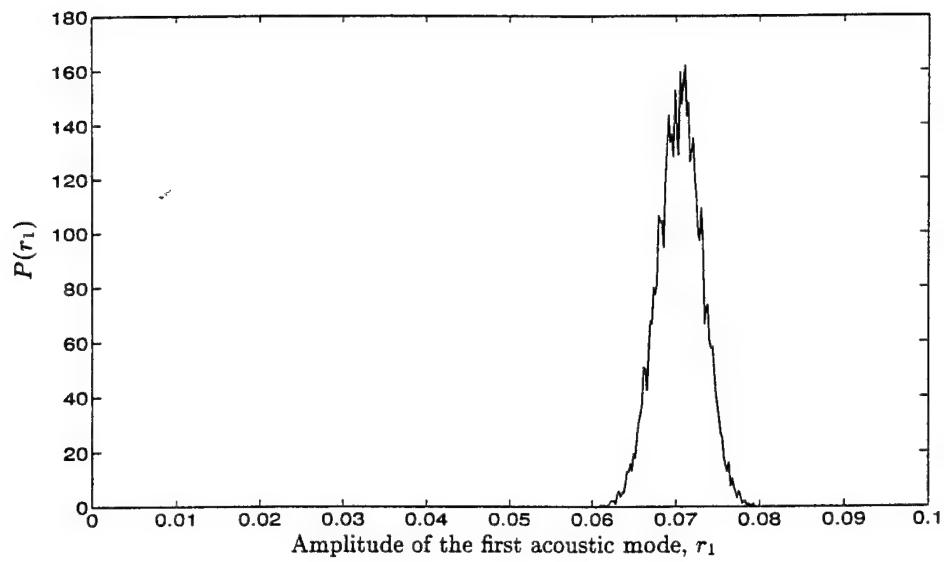
Figure 3: The influence of an external excitation of the fundamental mode only on a linearly unstable system; 2 modes, $\sigma_1^{\Xi} = 0.0005$ sec$^{-3/2}$, $\alpha_1 = 25$ sec^{-1}
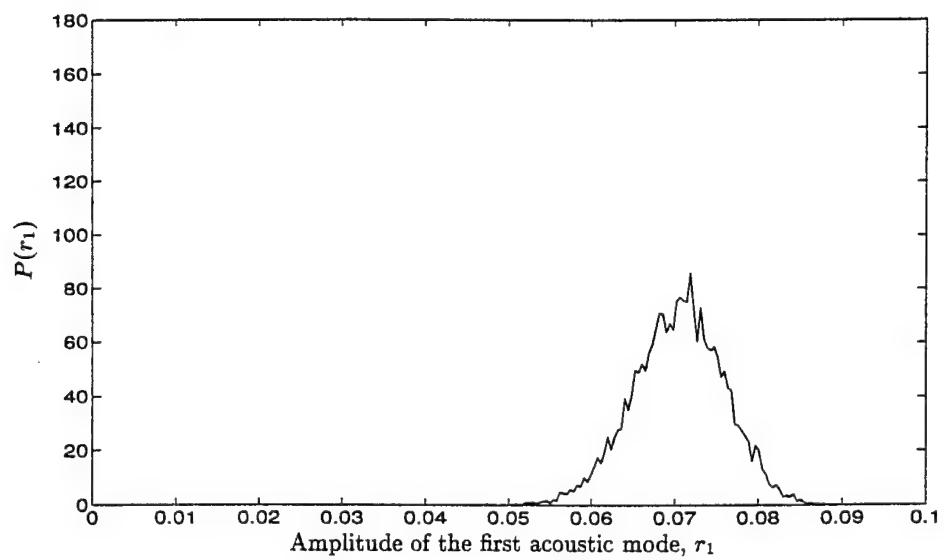
Figure 4: The influence of increasing the intensity of an external excitation of the fundamental mode only; 2 modes, $\sigma_1^{\Xi} = 0.001$ sec$^{-3/2}$, $\alpha_1 = 25$ sec^{-1}
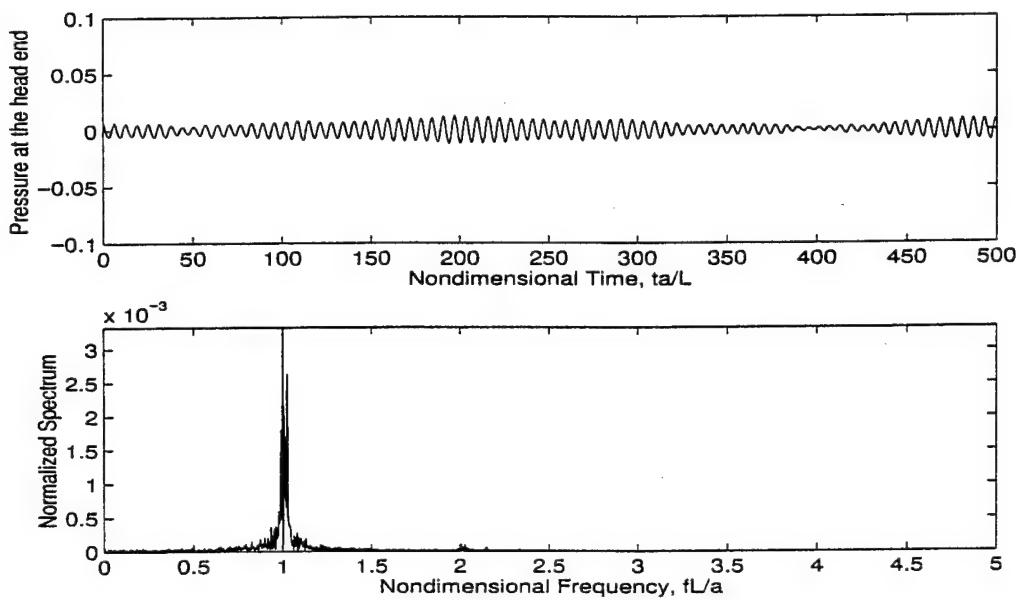
Figure 5: Sample pressure trace and spectrum for a simulation of a stable system with an external excitation; 2modes, $\sigma_1^{\bar{\Xi}} = 0.0005$ sec$^{-3/2}$, $\alpha_1 = -25$ sec^{-1}
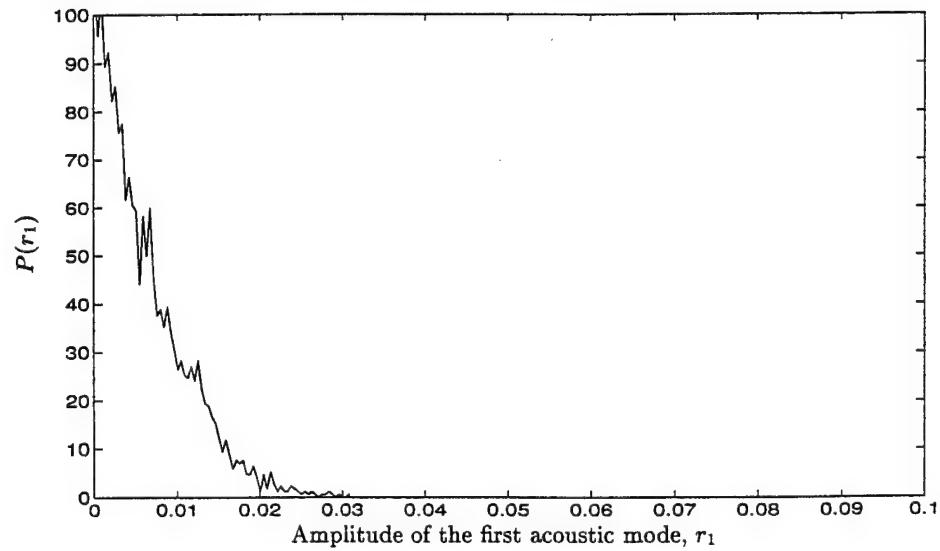
Figure 6: Probability density function for a system with a noisy linear growth rate in the fundamental mode only; 2 modes, $\sigma_1^{\xi^v} = 0.01$ sec$^{-3/2}$, $\alpha_1 = -8$ sec^{-1}

27
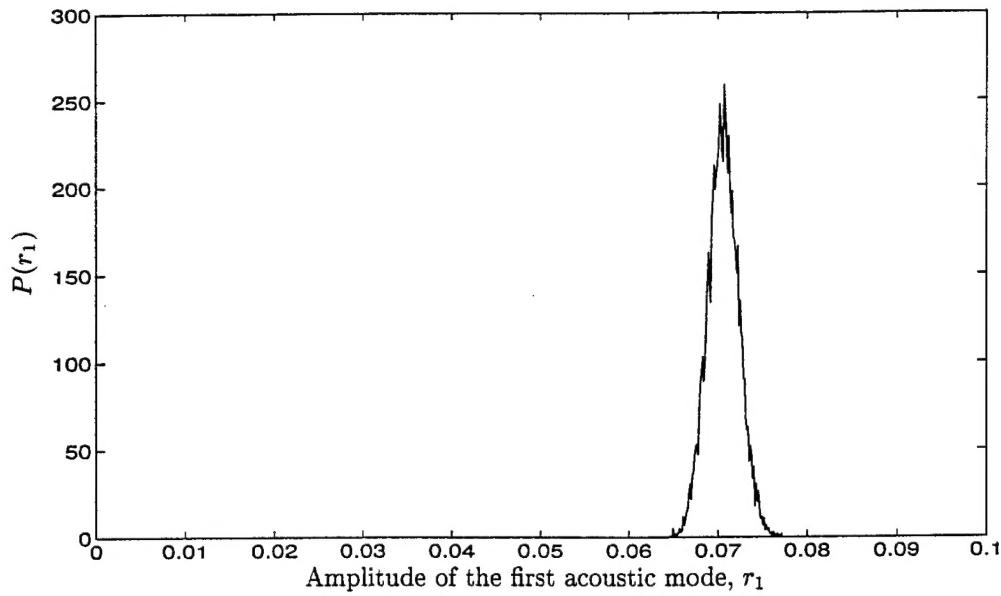
Figure 7: Probability density function for a system with a noisy linear growth rate in the fundamental mode only; 2 modes, $\sigma_1^{\xi^v} = 0.005 \text{ sec}^{-3/2}$, $\alpha_1 = 25 \text{ sec}^{-1}$
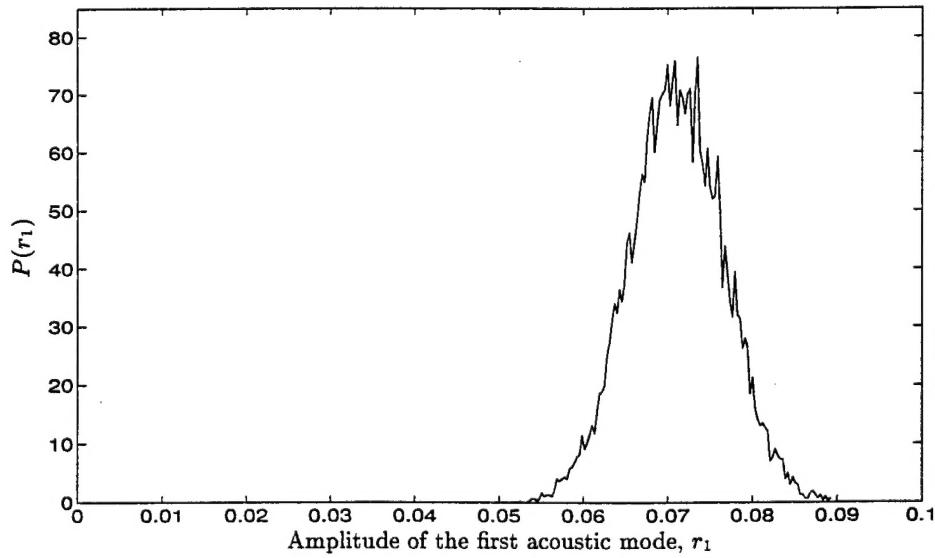
Figure 8: Probability density function for a system with a noisy linear frequency shift in the fundamental mode only; 2 modes, $\sigma_1^{\xi} = 0.025 \text{ sec}^{-1/2}$, $\alpha_1 = 25 \text{ sec}^{-1}$
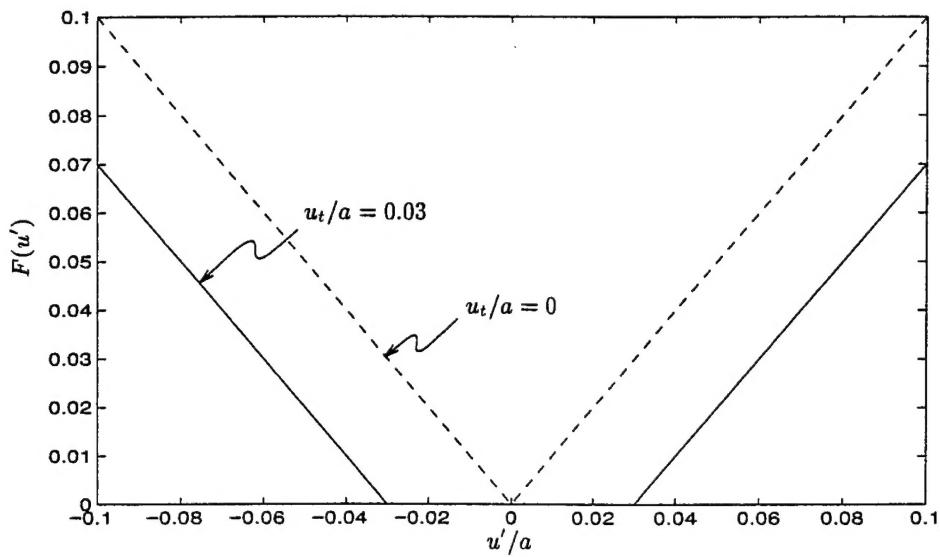
Figure 9: Threshold velocity function; $u_t/a = 0.03$
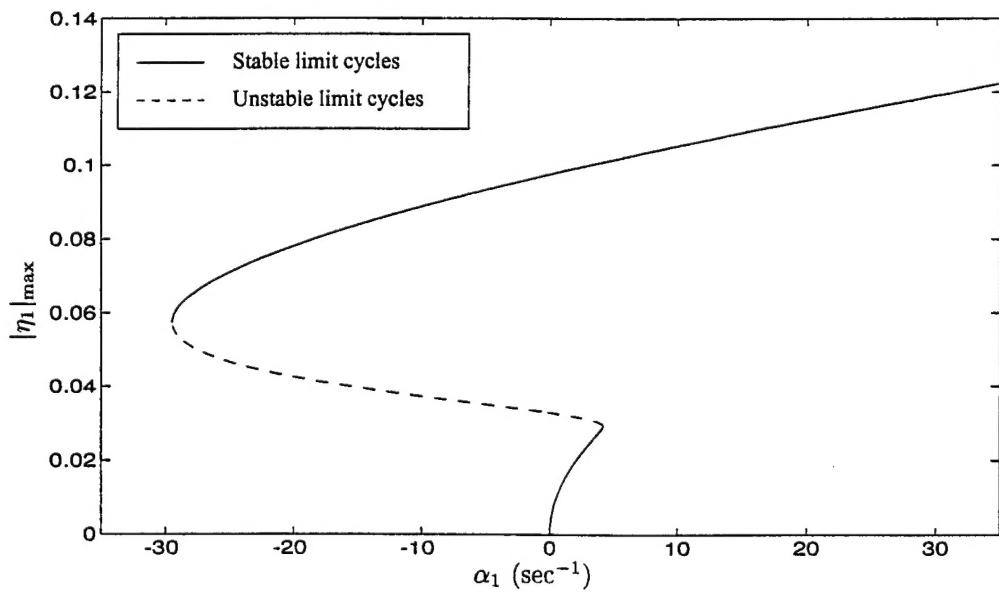
Figure 10: Bifurcation diagram for the deterministic system; threshold velocity model, $u_t/\bar{a} = 0.03$, $R_{vc} = 7.8$, 4 modes
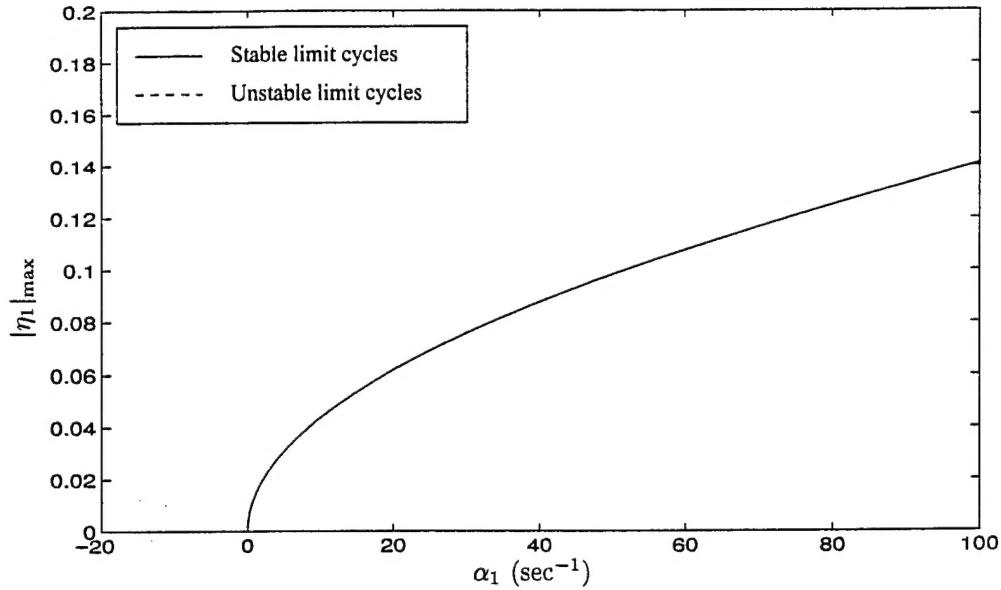
Figure 11: Bifurcation diagram for the deterministic system; 2 modes

(a) $\alpha_1 = -35$ sec^{-1}

(b) $\alpha_1 = -25$ sec^{-1}

(c) $\alpha_1 = -20$ sec^{-1}

(d) $\alpha_1 = -10$ sec^{-1}
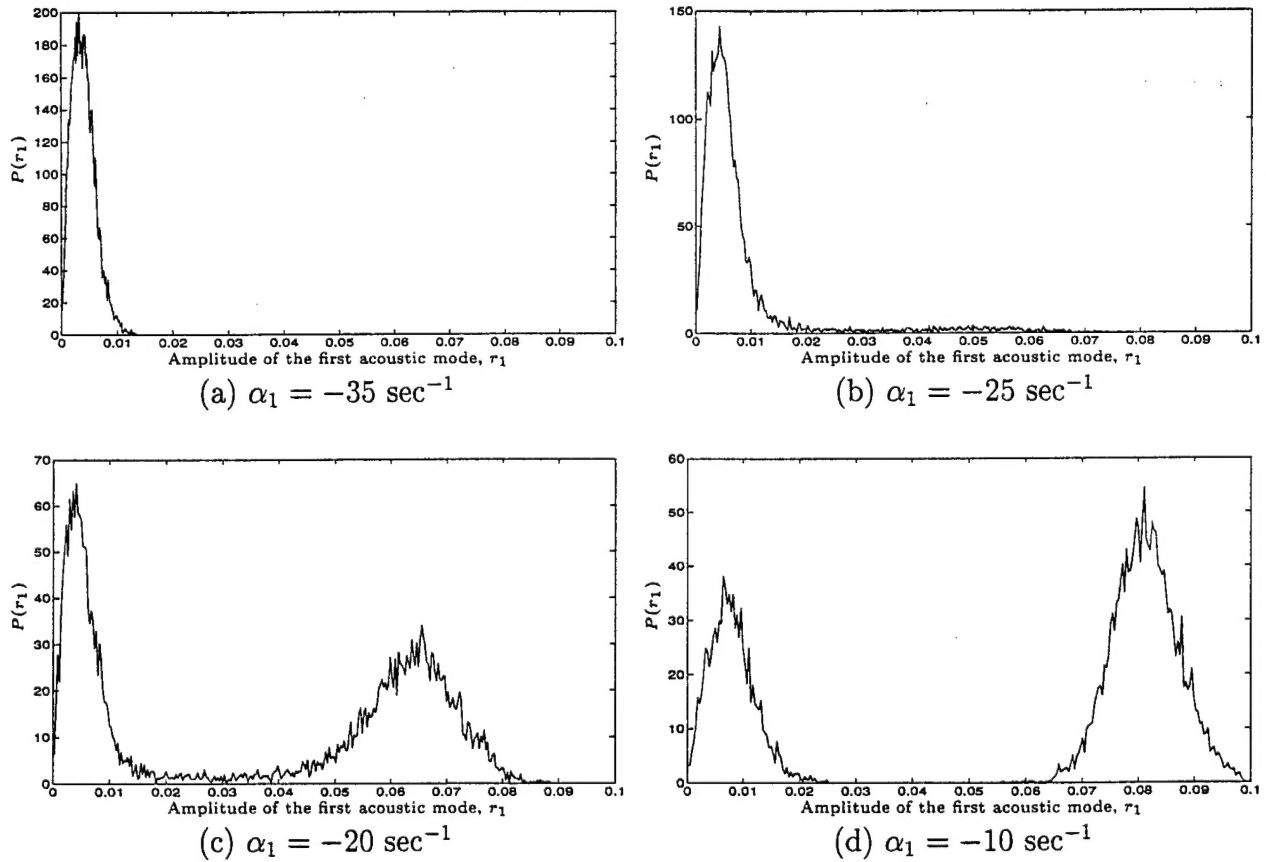
Figure 12: Probability density function of the first acoustic mode for various values of α_1; threshold velocity model, $u_t/\bar{a} = 0.03$, $R_{vc} = 7.8$, 4 modes

30

List of Figures